Vol. 56: 245–259, 2013
doi: 10.3354/cr01155

CLIMATE RESEARCH
Clim Res

Published online May 16

Extreme daily precipitation totals in Poland during summer: the role of regional atmospheric circulation

Michał Marosz[1,*], Robert Wójcik[1], Michał Pilarski[1], Mirosław Miętus[2]

[1]Institute of Meteorology and Water Management, National Research Institute, Podleśna 61, 01-673, Warszawa, Poland
[2]University of Gdańsk, Bażyńskiego 1a, 80-309, Gdańsk, Poland

ABSTRACT: The principal aim of the research was to describe the summer variability of extreme daily precipitation totals in Poland and to identify and quantify its relation to regional atmospheric circulation. The case of extreme precipitation was defined as a day with a daily precipitation total above the value of the long-term 90th percentile of daily precipitation totals (on a monthly scale). Spatio-temporal variability of extreme precipitation occurrences was investigated with the aid of eigentechniques, while identification of the relationship between regional forcing (atmospheric circulation) and local response (extreme daily precipitation occurrence) was attempted via redundancy analysis (RDA). The downscaling model was constructed on the basis of the 1971–1990 period and its verification comprised the periods 1961–1970 and 1991–2008. The variance of the local response to regional forcing explained by the RDA model exceeds 70% in the case of individual months and is nearly 60% in case of the whole summer season. However, the high number of identified empirical orthogonal functions (EOFs) suggests significant influence of local conditions on the spatial variability of extreme rainfall. Relatively high values of redundancy index (50 to 60%) also show that for individual months the variability of the sea level pressure (SLP) over the Euro-Atlantic region determines a substantial share of extreme rainfall. However, unsatisfactory results of model verification also imply that the connections established by the model might not be stationary, and that a longer period should be used in the model calibration process.

KEY WORDS: Precipitation extremes · Downscaling · Climate extremes

1. INTRODUCTION

The occurrence of extreme precipitation has brought about with remarkable frequency a number of significant losses in infrastructure, not to mention human tragedies. During the last 15 yr the catastrophic floods in July 1997 (Czech Republic, Poland), July–August 2001, (Poland), August 2002 (Czech Rep., Austria, Germany, Slovenia), August 2005 (Central and Eastern Europe), June 2009 (Czech Rep., Hungary, Poland and Romania) and May–June 2010 (Poland) highlight the need to investigate summer precipitation events in Central Europe, which are often extreme in terms of amount and intensity. This research focuses on the description of the spatial and temporal variability of extreme daily precipitation events in Poland during summer months (June, July and August; JJA). Also, it seeks to identify and quantify the relation of extreme precipitation events with regional atmospheric circulation by means of statistical-empirical downscaling. This may be useful in detecting the future trends in the occurrence of extreme events in combination with GCM climate simulations based on Intergovernmental Panel on Climate Change (IPCC) emission scenarios.

An extreme precipitation was defined (in accordance with IPCC guidelines) as the daily precipitation total exceeding the value of the long-term 90th percentile of the daily rainfall for individual months. This index cuts off the top 10% of daily precipitation

*Email: michal.marosz@imgw.pl

totals distribution and thus can be considered as an indicator of moderate climate extremes (Haylock & Goodess 2004). The chosen threshold is somewhat subjective; however one may find many examples of analogous usage of the long-term 90th percentile (e.g. Haylock & Goodess 2004, Haylock et al. 2006, Busuioc et al. 2008). This threshold was also used as an indicator of extreme precipitation during the STARDEX project (Statistical and Regional Dynamical Downscaling of Extremes for European Regions). In the case of Poland it may of course be argued that the 90th percentile is not suitable to indentify extreme events. This may stem from the assumption that a daily rainfall of 12 to 16 mm is not enough to be considered a precipitation extreme and it may include some events that are not extremes *per se*. However, the introduction of a higher threshold would result in a smaller amount of data to identify the relation between the regional and local meteorological fields. Therefore the chosen threshold of the 90th percentile of daily rainfall seems to be a reasonable compromise between defining extreme precipitation and ensuring enough data to calibrate the statistical model.

As many studies have already shown, statistical downscaling of precipitation extremes is a challenging task and rarely provides satisfying results (e.g. Harpham & Wilby 2005, Busuioc et al. 2008). With respect to precipitation, a systematic difference in performance between seasons is usually observed, and relatively low spatial coherence of such phenomena deteriorates the results especially during summer (Haylock at al. 2006, Goodess et al. 2012). The STARDEX project (Goodess et al. 2005) provided guidelines on the more robust methods for downscaling extremes, and stated that performance of statistical models in terms of precipitation extremes is generally 'poor', with the lowest skill in summer. Also, Haylock et al. (2006) found that although the worst results were achieved for summer, extreme rainfall occurrence was better modeled than its intensity. A variety of surface and upper-air predictors for downscaling winter extreme precipitation in Europe were examined by Haylock & Goodess (2004), and the best results were found for atmospheric pressure parameters such as sea level pressure (SLP).

Analyses of how atmospheric circulation influences extreme precipitation in Poland usually focus on the southern part of the country where considerably intense precipitation (with large totals) occurs relatively frequently. Examples of this are Twardosz (1999) and Zawiślak (2005), who both associate extreme precipitation with cyclonic circulation. Kolendowicz (2007) argued that the greatest influence on the occurrence of thunderstorm days is posed by the synoptic situation where a cold front passes from the western sector and a high pressure system is present east of Poland, resulting in the advection of warm and moist tropical air from the south. This suggests a direct relation between the shape of the regional SLP field and the occurrence of extreme precipitation events.

2. DATA AND METHODS

The occurrence of extreme precipitation was characterized by the monthly number of days with precipitation totals exceeding the long-term 90th percentile of daily precipitation (d_{90}). Based on the daily precipitation totals at 54 synoptic stations (Fig. 1) in Poland, d_{90} was estimated for summer months from 1961–2008. The values of the long-term 90th percentile for each station were calculated for the reference period 1971–1990 and only wet days (with rainfall of at least 0.1 mm) were taken into account. Precipitation data originate from the Institute of Meteorology and Water Management — National Research Institute (IMGW — NRI) database, which is verified and checked for homogeneity on a regular basis. There was no missing data in the model calibration (reference) period.

Some of the rain gauges we utilized in the research were also used during the European Climate Assessment (ECA) Project, and their (daily precipitation totals) homogeneity was additionally verified and confirmed (Klok & Klein Tank 2009).

By means of eigenfunction techniques the identification of major spatial patterns of variability of d_{90} was performed. The relationship between the regional atmospheric circulation and the occurrence of extreme precipitation in Poland was investigated using redundancy analysis (RDA), which is one of the methods of statistical downscaling procedures. A commonly used approach in the recognition of the relations between regional and local meteorological fields is canonical correlation analysis (CCA) (e.g. von Storch et al. 1993, Werner & von Storch 1993, Miętus 1999, Busuioc et al. 2001), which aims at the maximization of the correlation between the canonical time series. RDA, on the other hand, recognizes the patterns that are strongly connected by the regressive model: the first pair of maps explains maximum variance of the local field, the second, maximum from the leftover variance and so on (Miętus 1999).

Wang & Zwiers (2001) provide a neat explanation of the RDA method:

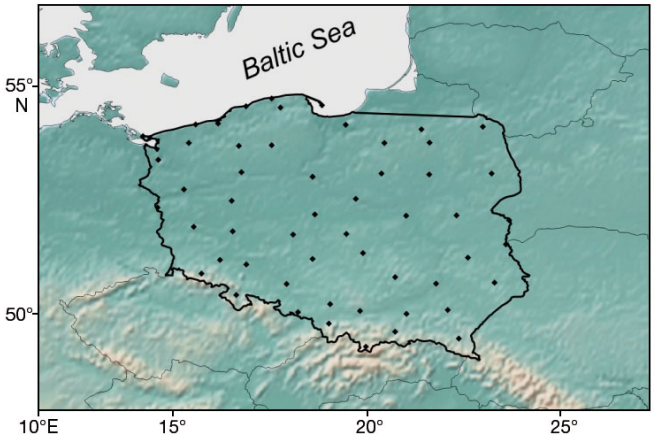

Fig. 1. Local variable response domain (Poland). Dots: rain gauges used in the study; colour: topography

Let **X** and **Y** be a pair of random vectors with dimensions M_X and M_Y, respectively. Also, let $\mathbf{R}_{XX}$ and $\mathbf{R}_{YY}$ be the covariance matrices of **X** and **Y**, respectively, and let $\mathbf{R}_{XY}$ and $\mathbf{R}_{YX}$ be their cross-covariance matrices. The regression of **Y** on **X** is given by:

$$\hat{\boldsymbol{Y}} = \mu_Y + \mathbf{R}_{XY}\mathbf{R}_{XX}^{-1}(\mathbf{X} - \mu_X) \quad (1)$$

where $\hat{\boldsymbol{Y}}$ is the linear prediction of **Y** that is obtained from **X**, and μ_X and μ_Y are the expected values of **X** and **Y**, respectively, which, without loss of generality, are hereafter taken to be zero; thus, the above equation reduces to:

$$\hat{\boldsymbol{Y}} = \mathbf{R}_{XY}\mathbf{R}_{XX}^{-1}\mathbf{X} \quad (2)$$

Once we have obtained the predictand estimates, $\hat{\boldsymbol{Y}}$, with the above regression equation, we can easily estimate the empirical orthogonal functions (EOFs) of $\hat{\boldsymbol{Y}}$ by solving the eigen-equation:

$$\mathbf{R}_{\hat{Y}\hat{Y}}\mathbf{a}_j = \lambda_j \mathbf{a}_j \quad (3)$$

where $\mathbf{a}_j$ and $\boldsymbol{\lambda}_j$ are ordered so that (for K dimensions) $\lambda_1 \geq \lambda_2 \geq \ldots \geq \lambda_K$. The first orthonormal mode $\mathbf{a}_1$ is the predictand mode best predicted by the regression model in the sense that it is the mode with the greatest variance. The second mode, $\mathbf{a}_2$, which is orthogonal to the first mode, is the second best-predicted mode, and so on. These best-predicted modes (also referred to as RDA modes) together form an orthonormal transformation $\mathbf{A} = [\mathbf{a}_1, \mathbf{a}_2, \ldots, \mathbf{a}_K]$. The jth best-predicted component is given by $\mathbf{a}_j^T\hat{\boldsymbol{Y}}$, and accounts for the jth largest proportion of the total predicted variance.

The full field that is forecasted with the regression model can be expanded in the RDA modes as:

$$\hat{\boldsymbol{Y}} = \mathbf{A}(\mathbf{A}^T\hat{\boldsymbol{Y}}) \quad (4)$$

These forecasts include high-order components $\mathbf{a}_j^T\hat{\boldsymbol{Y}}, j = K, K-1, \ldots,$ which may have very small redundancy indices, and thus, contribute little to forecast skill. Indeed, a cross-validated analysis of skill might reveal that it is prudent to include only a few of the low order predicted modes in the final forecast. An expression for a reduced forecast that includes only the first L predicted modes is obtained by replacing matrix **A** with a matrix that is composed only of the first L columns of **A**. The resulting expression for the reduced forecast is given by:

$$\hat{\boldsymbol{Y}}_R = \sum_{j=1}^{L}(\mathbf{a}_j^T\mathbf{Y})a_j \quad (5)$$

The best-predicted components can be readily expressed as linear combinations of the predictor. Specifically, $\mathbf{a}_j^T\hat{\boldsymbol{Y}} = \lambda_j^{1/2}\mathbf{b}_j^T\mathbf{X}$, where $\mathbf{b}j$ is given by:

$$\mathbf{b}_j = \lambda_j^{1/2}\mathbf{R}_{XX}^{-1}\mathbf{R}_{XY}\mathbf{a}_j \quad (6)$$

Substituting this into Eq. (5) shows that the reduced forecast based on the L best-predicted modes is given by:

$$\hat{\boldsymbol{Y}}_R = \sum_{j=1}^{L}\lambda_j^{1/2}(\mathbf{b}_j^T\mathbf{X})\mathbf{A}_j \quad (7)$$

The decomposition of the predictand field into RDA modes also results in an associated decomposition of the predictor field. Specifically, the predictor field can be expanded as $\mathbf{X} = \mathbf{P}(\mathbf{B}^T\mathbf{X})$ where $\mathbf{B}^T\mathbf{X}$ is the vector of predictor indices $\mathbf{b}_j{}^T\mathbf{X}$, and **P** is the matrix of adjoint patterns (predictor patterns) given by $\mathbf{P}^T = \mathbf{B}^{-1}$.

RDA seeks to find the best-predicted modes and the associated predictor patterns. That is, it allows us to associate a hierarchy of best-predicted orthogonal modes $\mathbf{a}_1$, $\mathbf{a}_2$, …, with the predictor patterns $\mathbf{p}_1$, $\mathbf{p}_2$, … that forecast these modes.

The redundancy index (R^2) determines the share of variance of a local field (predictand), which is explained by the variability of the regional field (predictor) (Miętus & Filipiak 2002). Its formal detailed description can be found in Wang & Zwiers (2001). CCA and RDA provide relatively similar outcomes in the case of low dimensional geophysical fields. The authors' opinion is that in the case of the element whose variability is usually described by a substantial number of EOFs, it is more appropriate to use the method providing clear identification of the local field variance. A detailed mathematical description of the RDA method can be found in Tyler (1982), von Storch &

Navarra (1999), von Storch & Zwiers (1999), and Makarenkov & Legendre (2002). This approach, however, has been relatively rarely used in climatology. The examples of redundancy method utilization in climatology and oceanography include Waves and Storms in the North Atlantic (WASA) project results (1998), Miętus (1999) and Miętus & Filipiak (2002). The WASA Group (1998) used RDA to perform backward reconstruction of wave height on the 2 oil fields in the Northeast Atlantic. The downscaling model related winter large-scale SLP and quantiles of significant wave height and showed a good reconstruction skill (in terms of correlation coefficient and explained variance). Subsequently the RDA was fed with 2 different time-slice experiments to produce empirical scenarios for possible future changes in storm surge. Wang & Zwiers (2001) showed the potential of RDA in statistically improving the skill of dynamical 500 hPa geopotential hindcast. The example of RDA application to different science fields was shown by Makarenkov & Legendre (2002); they presented a method of modifying RDA to express polynomial relationships instead of linear in classical RDA. Applied to real ecological data (abundance of hunting spiders versus environmental factors), the polynomial models accounted for greater total variance of the response variables than did linear RDA.

The regional atmospheric circulation (predictor) over the Euro-Atlantic region (35°–75° N, 50° W–40° E,) was characterized with an average monthly SLP field acquired from NCEP/NCAR reanalysis (Kalnay et al. 1996). The relation between the regional and local fields was established on the basis of the reference period (1971–1990). Calibrated redundancy models were subsequently verified with the data from the combined independent periods 1961–1970 and 1991–2008.

3. RESULTS

3.1 Spatio-temporal structure of extreme precipitation events

Annual average precipitation totals in Poland vary from <550 mm in the central part of the country to >1000 mm in the mountainous region (Tatra Mts.) in the south. Slightly elevated values are also encountered in the lake districts and the coastline of the Baltic Sea exceeding 700 mm. There is a marked domination of warm season (May to October) precipitation and its share in annual totals usually exceeds 60% in the central part of the country whereas in southern Poland this ratio may exceed 70% (Lorenc 2005), and intense summer precipitation is usually responsible for flood events.

Spatial variability of the average (1971 to 1990) value of the 90th percentile of daily precipitation totals shows relatively low diversity over lowland (northern and central) Poland, with values oscillating between 12 and 16 mm (Fig. 2). In general there is a slight tendency for values to increase towards the east. There are also isolated areas of values exceeding 16 mm in northern Poland (June). Substantially higher values are recorded in the southern part of the country (>20 mm), especially in the Carpathian Mts. Spatial variability of d_{90} during summer (Fig. 3) provides additional insight into the characteristics of extreme precipitation events in Poland. On average, d_{90} values vary between 1.2 d (Baltic Sea coast, June) to 2.0 d in southern Poland (Tatra Mts., June). A local maxima exceeds 1.6 d (July) over northern Poland hilly lake districts SW of the Gdansk Bay. This feature is quite consistent with the one noted in June (with values lower by 0.2 d). In August the highest values of d_{90} extend over northern Poland with top values exceeding 1.4 d. In central Poland the number of days with extreme daily precipitation is the lowest,

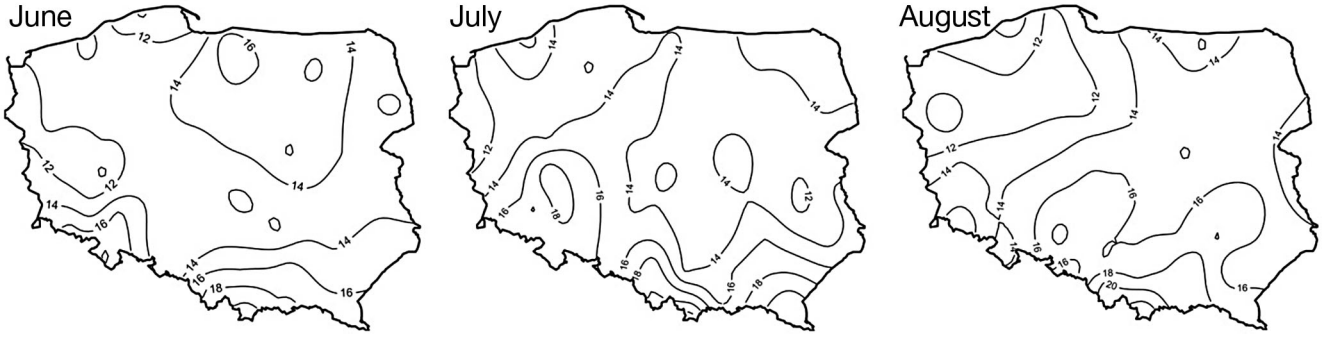

Fig. 2. Spatial variability of 90th percentile of daily precipitation totals (mm) during summer of 1971–1990: June, July and August

and in June it drops to <1.3 d. In July this area is shifted westwards. The spatial variability in August presents an area of values <1.2 d extending latitudinally across the country. During all summer months, the highest number of days with extreme precipitation is recorded in southern Poland in mountainous regions: the Tatra and Sudety Mts. The course of isolines suggests the gradual increase in d_{90} with increasing height.

Eigenfunction techniques allowed the investigation of the spatio-temporal variability of d_{90} (for the period 1961–2008). The number of non-degenerated EOFs (which explain >1% of d_{90} variance) is very high and ≥20 (Table 1) for all summer months, confirming high spatial variability in extreme precipitation occurrence and furthermore the complexity of its genesis. In total, non-degenerated EOFs explain >90% of d_{90} variance, with the highest value in June (92.3%). The first 3 EOFs explain >40% of d_{90} variance, with the highest value reached in July (52.4%). The first EOF, which explains from 20.8 (June) to 35.0% (July) of d_{90} variance, exhibits a uniform positive anomaly over Poland (Fig. 4). This indicates that the most important (but not clearly dominant) mode of spatial variability of the analyzed variable is connected with the processes at a regional scale. In June, a large part of the country's territory is covered with anomalies slightly exceeding +0.6 d. This situation is also apparent in the vicinity of the Gdansk Bay. The values of d_{90} anomalies drop slightly in the south-eastern part of the country. In July the spatial variability of the 1st EOF is more pronounced. The lowest values dropping <+0.2 d occupy the coast of the Baltic Sea, and as one enters the lake districts there is a sudden increase of up to +0.6 d. These values extend southwards in the western part of the country, and the +0.8 d contour line reaches the Silesia Lowland (south-western Poland). In the southern part of Poland, values exceed +0.8 d (locally >+1.4 d).

Table 1. Variance (%) explained by the first 3 EOFs of days with extreme precipitation (d_{90}) in Poland for 1961–2008

EOF	June	July	August
1	20.8	35.0	26.4
2	12.1	10.4	10.5
3	7.2	7.0	8.3
Total (1–3)	40.1	52.4	45.2
Total variance explained by non-degenerated EOFs	92.3	90.9	91.0
EOFs with explained variance >1%	23	20	21

The south-eastern part of the country exhibits a drop in anomalies with values <+0.4 d. August reveals lesser variability in the shape of anomalies of d_{90}. Most of Poland's territory is characterized by values >+0.6 d (though ≤+0.8). The western part of the country shows lower values of anomalies (<+0.4 d).

The second EOF (Fig. 4) explains from 10.4 (July) to 12.1% (June) of d_{90} variance. Its spatial variability is more diverse than for the 1st EOF, which suggests an increase in the local factors influence on the process of extreme precipitation generation. The general feature is the change of the sign of the d_{90} anomaly from west to east across the country. In June the range of the anomalies covers 1.4 d, with the lowest values falling <-0.6 d in north-western Poland and the highest (+0.8 d) in the south. A larger part of the country exhibits positive anomalies whereas negative anomalies are located in the north-west. In July there is a greater extent of negative anomalies with the lowest values <–0.6 d in the west. Generally, the western, northern and north-eastern parts of the country are characterized by negative anomalies but their range is between –0.2 and –0.6 d. Anomalies rise towards the south-east with the ridge extending from the Tatra Mountains towards the north-east. In

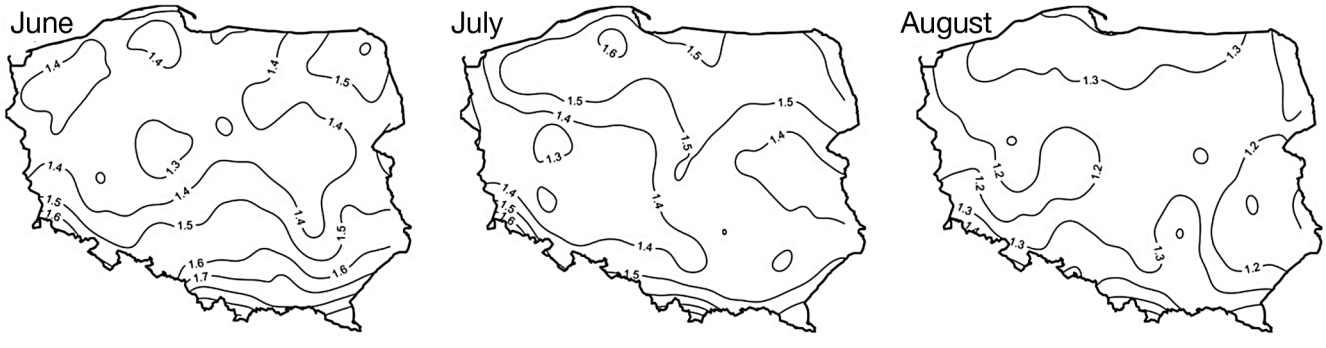

Fig. 3. Average values of days with extreme precipitation (d_{90}) during summer of 1971–1990: June, July and August

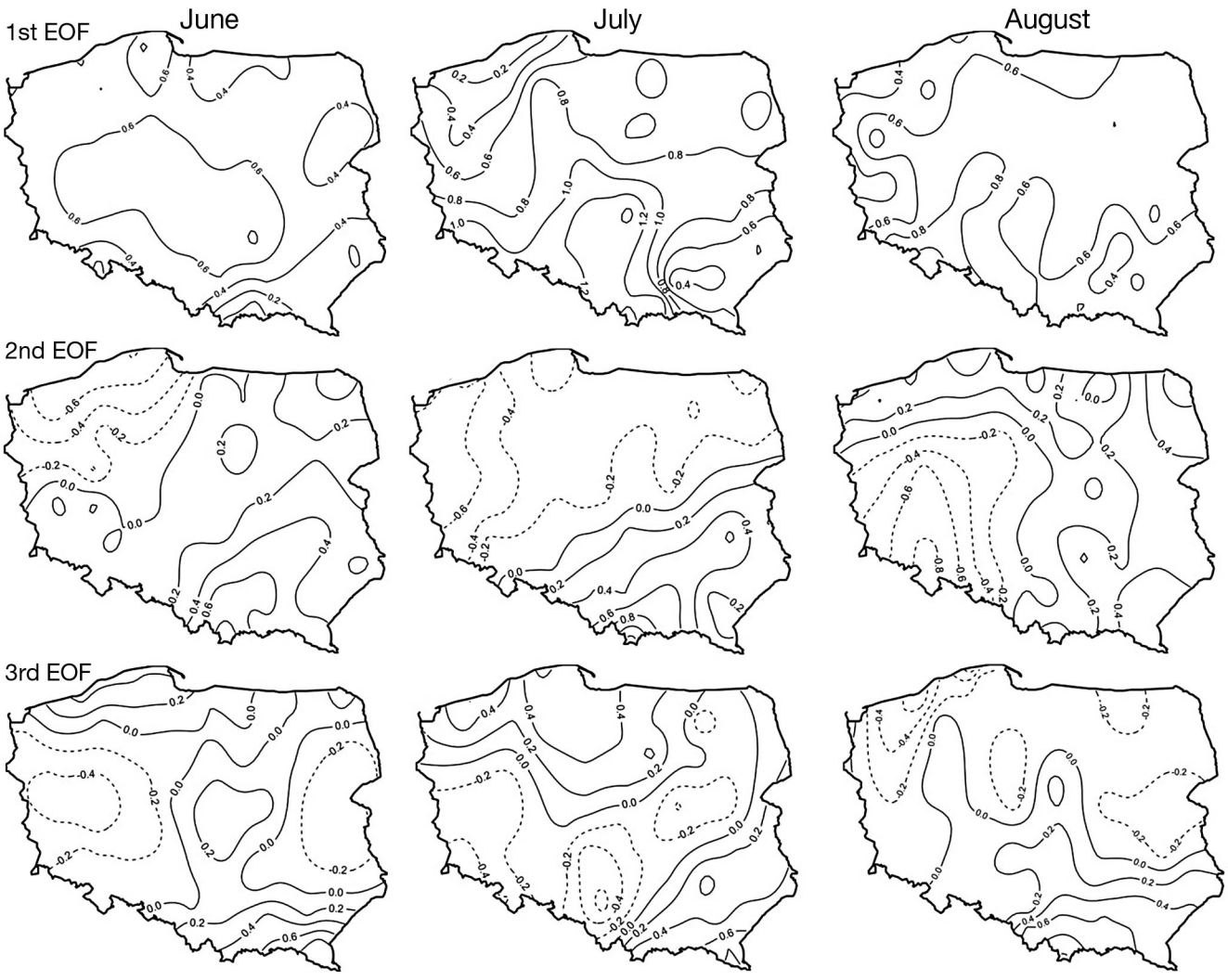

Fig. 4. Spatial variability (d_{90} anomalies, d) of the first 3 EOFs of days with extreme precipitation (d_{90}) in June, July and August 1961–2008

August negative anomalies are limited to the south-western part of the country, with the values increasing towards the Sudety Mts. reaching –0.9. The rest of the country exhibits positive anomalies, but the magnitude is somewhat smaller. The diverse sign of anomalies of the 2nd EOF can be attributed to smaller scale processes than those of the 1st EOF.

The 3rd EOF (Fig. 4) comprises from 7.0 (July) to 8.3% (August) of d_{90} variance. In the case of June, it shows positive anomalies (reaching +0.8 d) in the northern and southern parts of the country. The western and eastern areas are subject to negative anomalies divided by a weak ridge of positive values exceeding +0.2 d located in central Poland. The highest values of negative anomalies drop <–0.4 (west) and –0.2 d (east). In July there is a visible southward extension of the northern area of positive anomalies. In the coastal zone there is also an apparent increase in the values of the anomalies (>+0.6 d). The second area of positive anomalies occupies south-eastern Poland with values >+0.6 d. The region of negative anomalies is more coherent and stretches over the south-western and southern parts of the country with the visible extension into the NE direction. A positive sign of anomalies in northern and southern Poland in the case of June and July possibly shows the enhancing role of orographic barriers. The major change in the shape of the anomaly field in August in the case of the 3rd EOF marks the dominance of negative anomalies in northern Poland. The trough of negative anomalies extends southwards in western Poland. Positive anomalies >+0.8 d cover the southern part of Poland.

The course of the d_{90} principle components (PCs) oes not exhibit statistically significant trends with the exception of the 3rd EOF in August (Table 2). However, it is worth noticing that peaks of PCs (not shown) correspond closely with the occurrence of some of the largest precipitation floods recorded in Poland during the analyzed period. This applies to June (1999), July (1997) and August (1972, 2006). Those catastrophic events were usually connected with intense and prolonged rainfall (Dobrowolski et al. 2005, Dubicki et al. 1999, Grela et al. 1999). Generally, there is a marked domination of negative tendencies in PCs courses, which corresponds with the results of Łupikasza (2010) who investigated the recent trends in spatial and temporal variability of extreme precipitation in Poland. Łupikasza concluded that decreasing trends (1951–2006) in extreme precipitation indices are a dominant feature in the summer season, especially in the southern part of Poland. This is coherent with the spatial distribution of trends (1958–2000) in Europe presented by Haylock & Goodess (2004).

3.2. RDA model

The extreme precipitation events in summer are usually connected with rarely occurring (not dominant) patterns in the SLP field. Thus, all available data (i.e. derived non-degenerated SLP EOFs) were used in order to cover the most of SLP variability explained by RDA models. The downscaling model constructed by means of RDA resulted in 9 redundancy pairs for June and July and 8 for August (Table 3). The total amount of explained variance of the regional SLP field exceeds 90% for individual months. In the case of the local field (i.e. d_{90}), explained variance exceeds 70% (in total) for each of summer months with the highest values reached in August (76.88%). The redundancy index (R^2) determining the amount of variance of local field explained by the variability of regional forcing is 67% in July and 63% in June, whereas the lowest value occurs in August (57%). In the case of an RDA model for the whole summer season (JJA all together, not shown in the text) the R^2 is considerably lower (28.34%), which supports the hypothesis of varying origin (based on the regional air flow as its determinant) of extreme precipitation during summer months.

Table 2. Trend coefficients of EOFs (1st to 3rd) of days with extreme precipitation (d_{90}) (per 10 yr) for 1961–2008. *0.05 significance level of trend model

	1st	2nd	3rd
June	−0.128	−0.134	0.046
July	0.051	−0.037	−0.040
August	−0.040	0.022	−0.233*

Table 3. RDA model characteristics: variance (%) of regional (varSLP) and local (vard_{90}) fields explained by consecutive redundancy map pairs, redundancy index (R^2) and correlation coefficient (r) between the associated time series of regional sea level pressure (SLP) field and days with extreme precipitation (d_{90}) in Poland, 1971–1990

	r	varSLP	vard_{90}	R^2
1				
June	0.93	16.58	22.18	19.18
July	0.94	10.20	29.83	26.36
August	0.82	18.07	35.79	24.07
2				
June	0.98	6.57	15.65	15.03
July	0.98	8.44	11.04	10.60
August	0.95	5.14	12.67	11.43
3				
June	0.98	6.15	10.06	9.66
July	0.98	14.42	6.67	6.41
August	0.91	5.74	8.68	7.19
4				
June	0.98	22.72	5.54	5.32
July	0.98	22.74	5.90	5.67
August	0.92	23.78	5.67	4.71
5				
June	0.96	11.60	5.15	4.75
July	0.96	13.52	5.26	4.85
August	0.87	4.15	4.72	3.57
6				
June	0.95	10.16	4.93	4.45
July	0.98	8.75	4.32	4.15
August	0.93	4.79	3.69	3.19
7				
June	0.97	4.39	2.73	2.57
July	0.97	7.22	4.28	4.03
August	0.84	15.64	2.61	1.84
8				
June	0.71	8.74	3.04	1.53
July	0.88	4.85	4.00	3.10
August	0.72	19.54	3.15	1.63
9				
June	0.54	10.26	4.00	1.17
July	0.97	6.06	2.15	2.02
August	–	–	–	–
Σ				
June		97.17	73.28	63.66
July		96.20	73.45	67.18
August		96.85	76.88	57.64

The first 3 pairs of RDA maps explain >45% of d_{90} variance (Table 3) with the highest values in August (57.14%): 35.79, 12.67 and 8.68% for consecutive pairs. The values of correlation coefficients between the time series associated with the first 3 pairs of redundancy maps are very high, and with the exception of the 1st pair in August (0.82), they all exceed 0.9, implying a strong temporal relationship between derived patterns of regional and local elements (though the relatively low amount of explained variance may indicate the low skill of the model).

The first RDA map pairs explain from 10.20% (July) to 18.07% (August) of regional SLP field variability over the area of research and from 22.18% (June) up to 35.79% (August) of d_{90} variance. They are relatively similar for all summer months (Fig. 5). The common feature is a vast area of negative anomalies of SLP dominating over the whole regional forcing domain. The difference for individual months is the location of its centre: the Baltic Straits in June (Fig. 5a), which then shifts westwards in July (Fig. 5c). The ongoing westward shift in August (Fig. 5e) is less pronounced than in the June/July transition and the strength of the negative anomalies centre weakens. The resulting local element field anomalies (Fig. 5b,d,f) exhibit a generally positive response to the intensification of cyclonic circulation with the highest values of d_{90} anomalies located in north-western Poland (>+1.0 d) with a drop while moving south-east and east. It is most pronounced in June (Fig. 5b), and while transiting to consecutive months the area of the highest positive anomalies moves east: in July (Fig. 5d) it is located in north-eastern Poland while in August (Fig. 5f) in the south-eastern part of the country. Overall, the local field response is quite coherent and there are only isolated areas of negative anomalies. The existence of the highest negative SLP anomalies over the Baltic Straits and then over the North Sea could be linked with the frequent passing of low pressure systems intensifying the advection from the south or south-east and thus bringing warm air that is prone to produce intense rainfall when in contact with cooler air from over the Atlantic Ocean. The first RDA pair of patterns suggests that extreme precipitation occurrence in Poland is usually linked to cyclonic circulation, and this is consistent with conclusions of Twardosz (1999) and Zawiślak (2005).

The second RDA map pairs (Fig. 6) explain from 5.14 (August) to 8.44% (June) of regional SLP field variance and from 11.04 (July) to 15.65% (June) of d_{90} variability. The derived SLP patterns suggest the increase of importance of the advection from the east over Poland (June, Fig. 6a; July, Fig. 6c) and from the south-east (August, Fig. 6e) connected with the positive SLP anomalies (>+1.5 hPa) north-east of Poland (June) or a ridge of positive anomalies extending westwards over Scandinavia (July). In the case of August this is also accompanied by the well developed negative anomalies area west of the British Isles, which strengthens the southern advection. The corresponding spatial patterns of Δd_{90} over Poland reveal more pronounced variability, and the response of the local field is less coherent as there are areas with different signs of anomalies. In June (Fig. 6b) positive anomalies of d_{90} cover the majority of the country with the ridge of highest values (>+0.6 d) extending from the Tatra Mountains towards N-NE. The Baltic Sea coast and adjacent lake districts (NW Poland) are the areas of the negative d_{90} response, with the values of Δd_{90} dropping <–0.6 d in Łeba on the coast of the Baltic Sea. In July (Fig. 6d) there is an apparent extension of this area with an additional trough reaching Torun and Warsaw in the central part of the country. The positive response of d_{90} is confined to southern and eastern Poland, with values exceeding +0.6 d in Lublin. In August (Fig. 6f) the resulting Δd_{90} field reveals the change in the course of zero anomaly contour line, which divides the country into the western and eastern parts, which are respectively subject to positive (>+1.0 d) and negative (<–0.4 d) responses. The exception from this rule occurs on the Baltic Sea coast, which is characterized by a negative response of d_{90}.

The third RDA map pairs (Fig. 7) explain from 5.70% (August) to 14.42% (July) of the regional SLP field and from 6.67% (July) to 10.06% (June) of variability of d_{90}. The attained SLP patterns do not pose a coherent picture as in the case of the 1st and 2nd RDA pairs, and the transition between months does not show much continuity. In June (Fig. 7a) the SLP pattern results in the intensification of the flow from the N and NW over Poland, which is additionally strengthened by the presence of strong positive SLP anomalies centred over the North Atlantic. The resulting d_{90} pattern (Fig. 7b) explains >10% of variance of this element with negative anomalies >–0.3 d in the centre of Poland. The negative response of the d_{90} field also occurs in the coastal zone. The eastern part of the country is dominated by positive anomalies exceeding 0.6 d. Slightly less pronounced (0.4 d) d_{90} anomalies spread from the west via northern lake districts in a NE direction. July's SLP (3rd RDA pattern, Fig. 7c) explaining 14.42% of its variance exhibits a belt of negative anomalies stretching from the North Atlantic eastward, with values of <–1.5 hPa. Over the area of Poland, such an SLP anomaly is associated

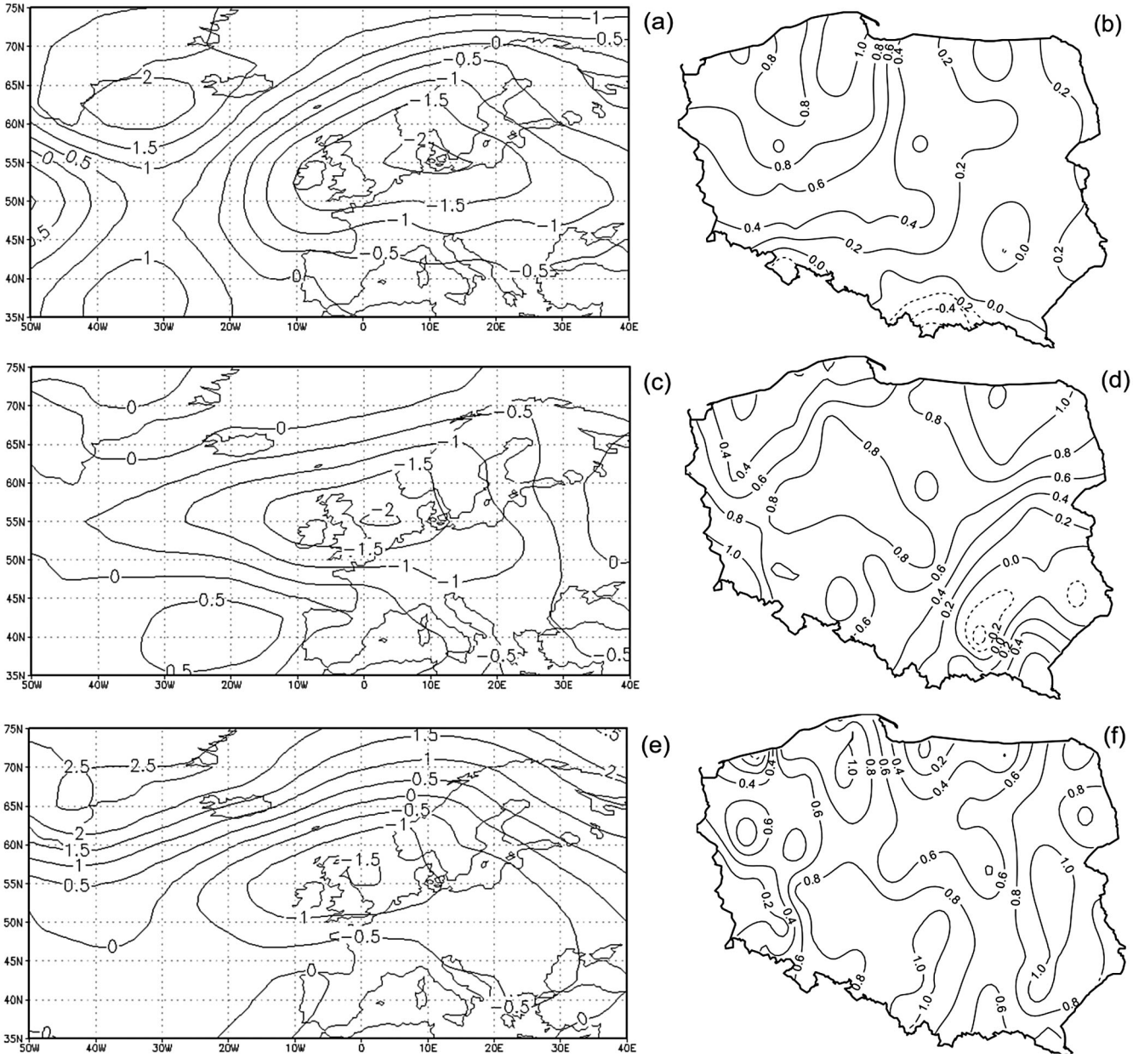

Fig. 5. First pair of redundancy maps between sea level pressure (SLP) (left; units: hPa) and days with extreme precipitation (d_{90}) (right; units: d) in Poland for (a,b) June, (c,d) July and (e,f) August 1971–1990, expressed in unit anomalies

with the d_{90} response (Fig. 7d) that shows a vast area of positive anomalies covering northern and eastern parts of the country. The highest anomalies reach +0.6 d. The situation in August is somewhat similar, i.e. the SW flow intensifies and the axis of a parallel belt of negative SLP anomalies is rotated by ~45° counterclockwise, now stretching from the Azores towards the NE (Fig. 7e). This SLP pattern explains 5.74% of variance, and the associated pattern of d_{90} anomalies explains 8.68% of its variance. The shape of the anomalies shows a positive response in the NE and SE parts of the country and a negative one in the east. Also, western and coastal parts of Poland are subject to a negative d_{90} field response (Fig. 7f).

3.3. RDA model validation

The RDA model was verified by calculating the correlation coefficients between observed and reconstructed d_{90} time series and values of Root Mean Square Error (RMSE) of the model. The procedure

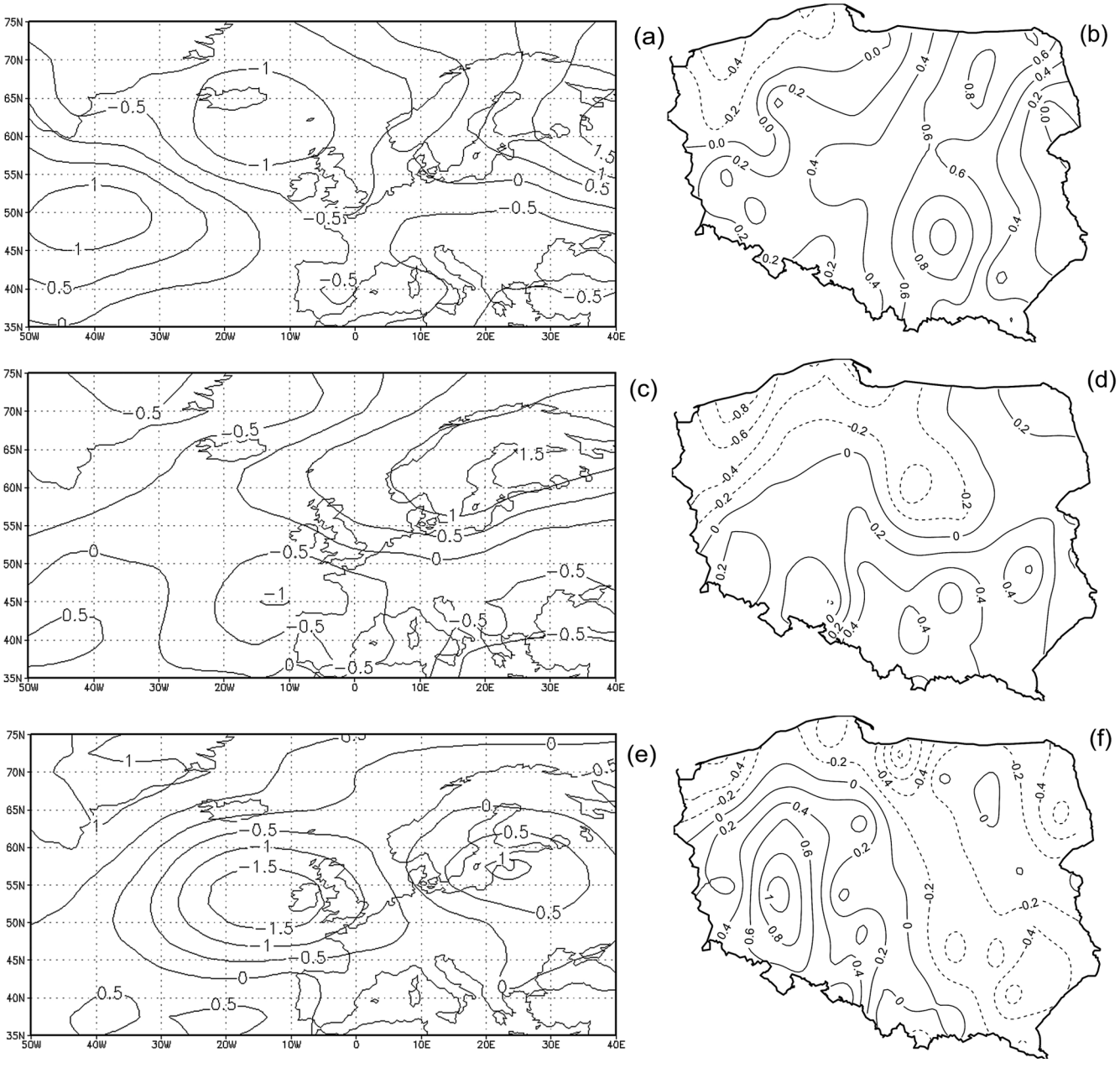

Fig. 6. Second pair of redundancy maps between (left) SLP and (right) d_{90} for (a,b) June, (c,d) July and (e,f) August 1971–1990. See Fig. 5 for details

was performed for the calibration period (1971–1990) and then for the remaining verification period (1961–1970 and 1991–2008). The comparison of calibration and validation periods shows (Fig. 8) that there is a large discrepancy in the values of correlation coefficients. For the calibration period, area average correlation coefficients for consecutive summer months are relatively high and equal: 0.73, 0.74 and 0.65 respectively. The ranges are 0.33–0.90 (June), 0.45–0.91 (July) and 0.46–0.82 (August). This suggests that extreme precipitation can be modeled via utilization of downscaling techniques such as RDA. However, the verification period provides significantly less encouraging results, with the average correlation coefficients value not exceeding 0.15: They are 0.12 (June), 0.08 (July) and 0.14 (August). The ranges are –0.39 to 0.61 (June), –0.51 to 0.57 (July) and –0.29 to 0.72 (August).

Analysis of RMSE variability (Fig. 9) seems to confirm the above mentioned discrepancies between the calibration and verification periods. For the calibration period, area average RMSE values equal

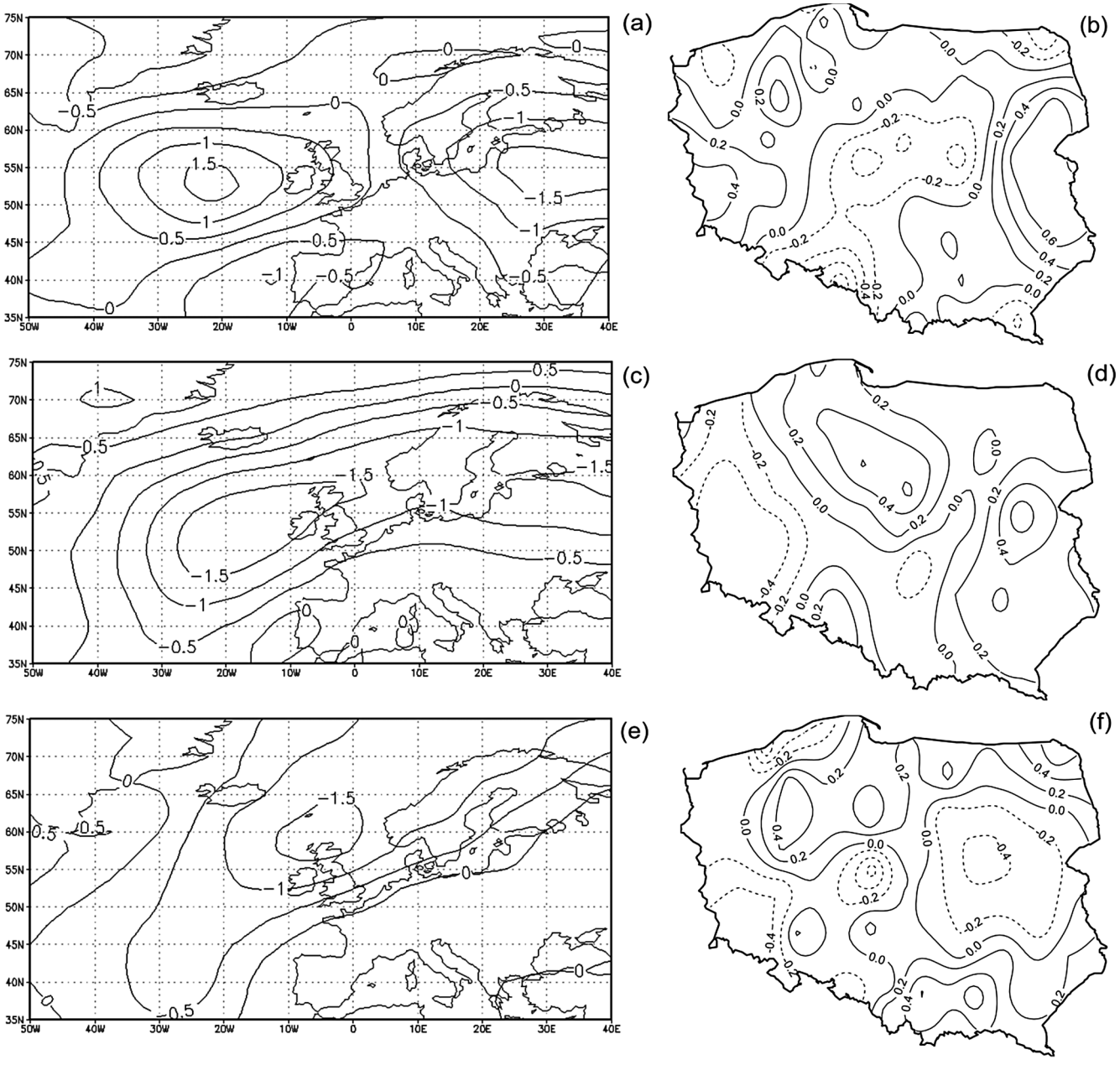

Fig. 7. Third pair of redundancy maps between (left) SLP and (right) d_{90} for (a,b) June, (c,d) July and (e,f) August 1971–1990. See Fig. 5 for details

0.79, 0.82 and 0.96 for consecutive summer months. The ranges are 0.47–1.25 (June), 0.50–1.31 (July) and 0.51–1.45 (August). The spatial RMSE variability in the calibration period is not highly pronounced, and in June and July it usually oscillates around 0.75, rarely exceeding 1.0 (northern Poland for the case of June). The value of 1.0 is also exceeded in the southern areas, but it is more pronounced in July. In August the values are on average 0.25 higher, and locally exceed 1.25. The verification period exhibits RMSE values around 2 times greater than those in the calibration period. The worst model quality is noted for July, with an average RMSE of 2.03, and the highest values exceeding 3 in the southwest part of the country. For June and August, average RMSE values are 1.64 and 1.63, respectively. Such an outcome may imply that the identified relations are not stationary, and the verification of the model is successful only for a couple of stations with relatively high correlation coefficients; thus, its applicability as a whole for the area of Poland is questionable.

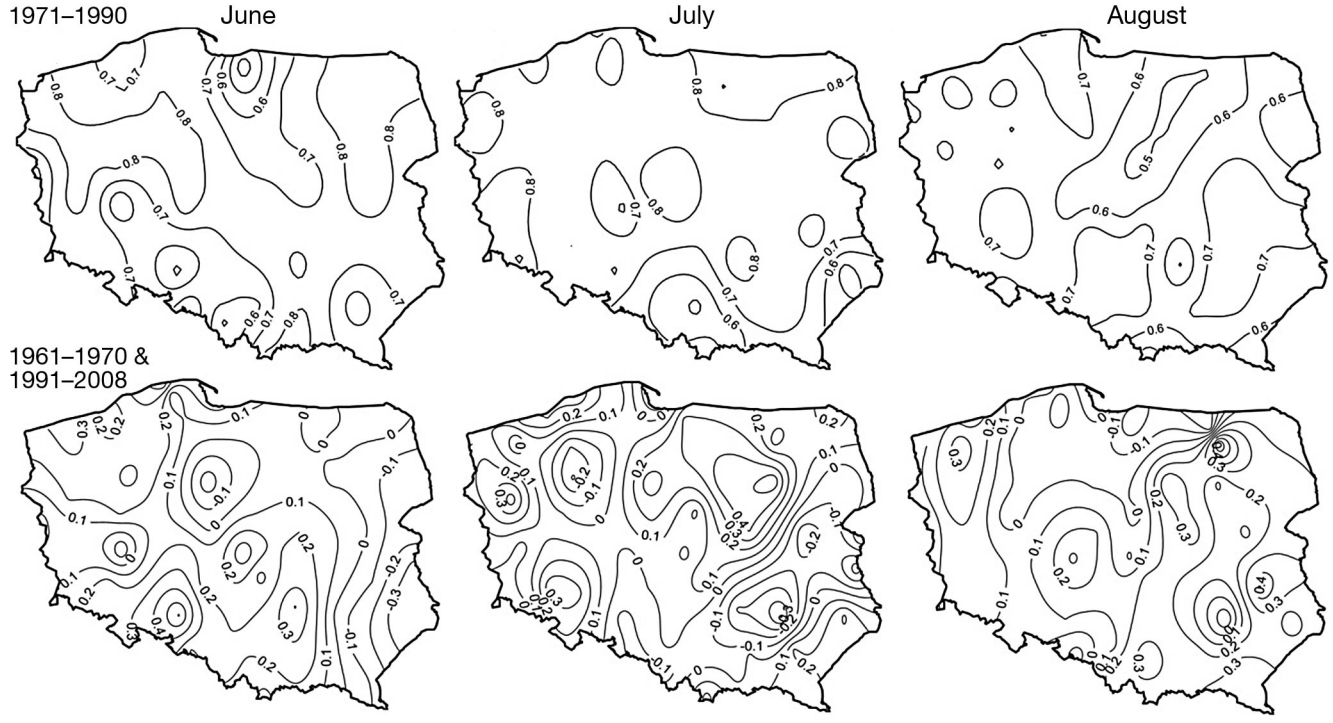

Fig. 8. Correlation coefficients between observed and reconstructed time series of days with extreme precipitation (d_{90}) for calibration (1971–1990) and verification (1961–1970 and 1991–2008) periods in June, July and August

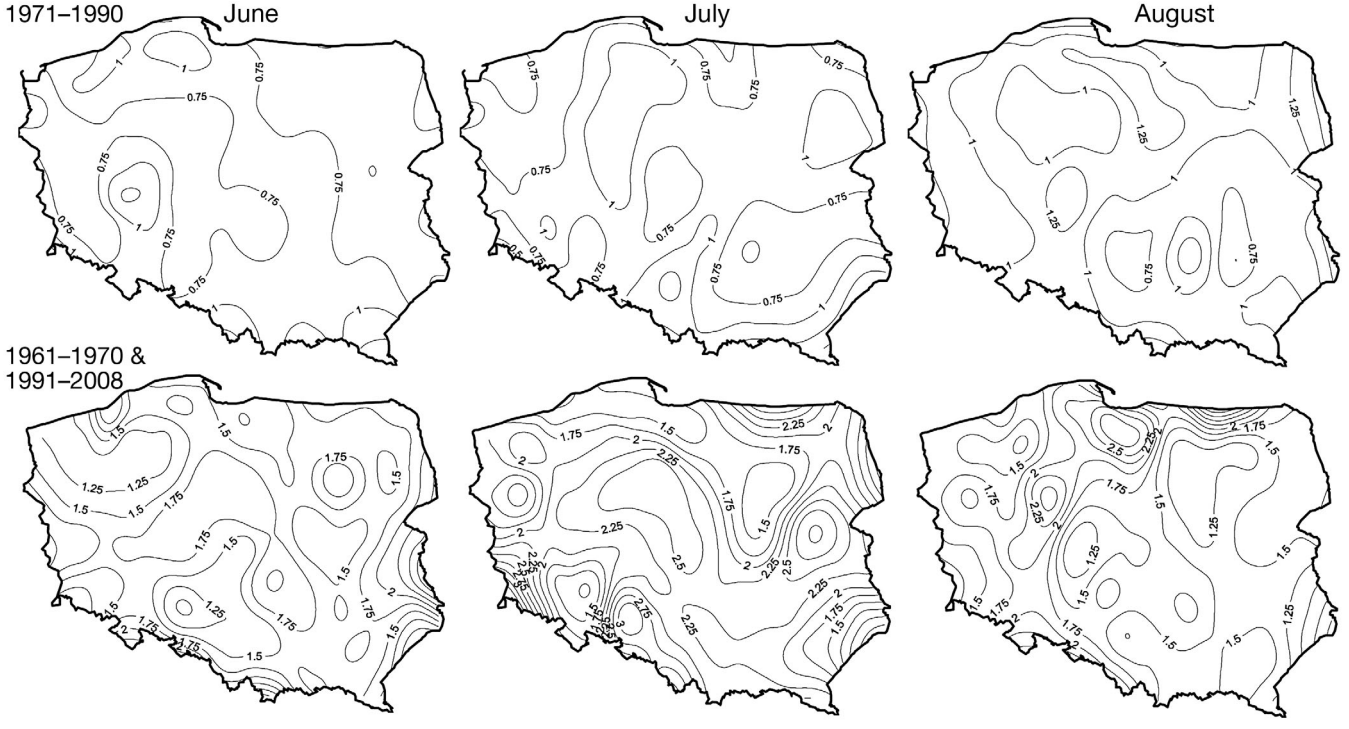

Fig. 9. RMSE (in d) of RDA models of d_{90} for calibration and verification periods in June, July and August. See Fig. 8 for details

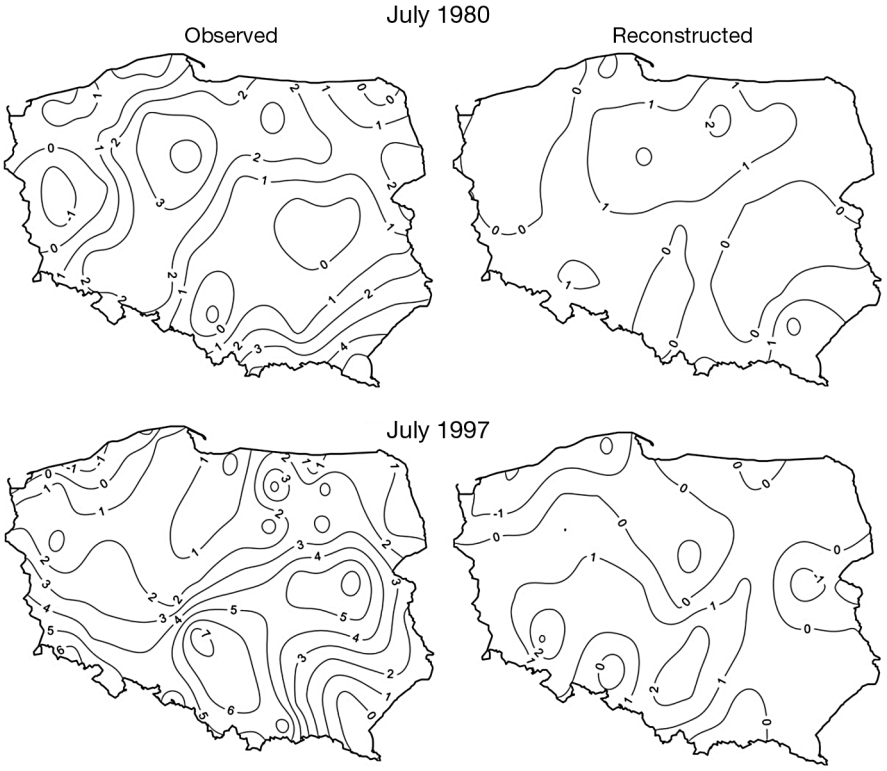

Fig. 10. Comparison of observed versus reconstructed (via RDA downscaling) days with extreme precipitation (d_{90}) for 2 months with catastrophic precipitation floods in Poland: July 1980 and 1997

The verification was also performed for selected situations of extreme precipitation in Poland: July 1980 and 1997 (Fig. 10). The results show substantial underestimation of the d_{90} values in both cases. Slightly better results are attained in the case of the event from the calibration period: the underestimation does not exceed 3 d (Fig. 10), whereas in the case of the 'millennium flood' in July 1997, the underestimation is much higher (Fig. 10). Also, the spatial patterns of reconstructed events do not match the observed spatial variability of d_{90}, especially for July 1997.

4. DISCUSSION

The results of statistical downscaling of extreme precipitation events occurrence during summer months in Poland do not meet some of the STARDEX robustness criteria (Goodess et al. 2005): strength and stability of relationships and uniformity of performance (across stations and time periods). A number of reasons are responsible for a low skill of the presented RDA model. The extreme nature of the analyzed phenomena is manifested with a small average d_{90} (~1.5 d mo^{-1}); moreover extreme precipitation events (according to the definition in this study) do not occur every month: in the 20 yr reference period at a country scale, such events were on average recorded in ~15 Junes, 15 Julys and 13 times in August, and for some stations this number did not exceed 10 to 12 events. Thus, the RDA model, designed to be trained on 20 yr series, was in fact calibrated on a somewhat smaller number of data, which may have affected its performance. A solution to this problem would incorporate the extension of the calibrating period. This however, would be limited by the need to have sufficient independent data for the subsequent model validation. Another way of increasing the number of data for model calibration purposes is to reduce the threshold of extreme precipitation to e.g. the 80th or even 70th percentile, but in such a case the definition of extremes would be clearly downgraded. The low sensitivity of the model based on monthly data is, to a large extent, a result of averaging the predictor over dry, wet and extremely wet days (Buishand et al. 2004); thus the signal of extreme events in the monthly predictor field can be questionable. To avoid this discrepancy, it would be appropriate to apply a statistical downscaling procedure to daily data, e.g. only to selected days when precipitation exceeding the given threshold was recorded. Such an approach would be useful in identifying direct relationships, since the linkages between SLP and precipitation have more physical sense on a daily scale. However, the aim of our research could not be accomplished with this approach, as the influence of the regional forcing on occurrence of a given phenomena in downscaling procedures should be considered while integrating through a certain time scale (in this case monthly). Daily values could be used to interrelate individual SLP patterns and precipitation totals (analog downscaling method), which was not the purpose of the investigation in this case. Another reason for rela-

tively poor model skill may be associated with predictor selection. Numerous studies concerning precipitation have proved that different predictors (other than SLP) could be of great importance, e.g. geopotential heights, wind components, vorticity, divergence, air humidity, vertical instability and even air temperature or SST (e.g. Wilby & Wigley 2000, Cavazos & Hewitson 2005, Harpham & Wilby 2005, Schmith 2008; Sauter & Venema 2011). An assessment of potential predictors for downscaling precipitation in Poland has yet to be undertaken.

The analyzed index of extreme precipitation occurrence is characterized by considerable spatial incoherency (~20 EOFs), giving evidence of a complicated origin of extreme precipitation events. Using regional indices (e.g. for the area averaged d_{90})would possibly help solve this inconvenience.

On the basis of the above considerations, the merits of the presented RDA model are arguable. However, it should be noted that the skill of this RDA model is comparable to other linear multivariate methods applied to extreme precipitation occurrence in summer, e.g. for the United Kingdom (Haylock et al. 2006). The lowest skill for southern Poland suggests that in mountainous areas other factors (e.g. potential instability; Busuioc et al. 2008) play a more important role.

5. CONCLUSIONS

A very large number of EOFs of d_{90} indicates the considerable share of local factors in shaping the spatial variability of this phenomenon over Poland. On the other hand, a coherent d_{90} anomalies field of the first RDA pattern suggests that macroscale atmospheric circulation may be an important factor posing favorable/unfavorable conditions for the occurrence of extreme precipitation. Yet, the occurrence of the event itself might — to a considerable degree — be determined by local conditions such as relief, land use or active surface temperature. Our results (e.g. redundancy index) suggest that the variability of the regional SLP field over the North Atlantic and Europe accounts for 57 (August) to 67% (June) of d_{90} variance during individual summer months, whereas for the RDA model constructed for the whole season (JJA) the index is <30%. Those results imply that in individual months of the summer season, the occurrence of extreme daily precipitation totals is stimulated by distinct patterns of the SLP field. Most of the variance of d_{90} (1st RDA map pair) is connected with a vast negative anomaly located in the vicinity of the North Sea. The resulting d_{90} anomalies in Poland are coherent in terms of the response to regional forcing. The consecutive RDA map pairs present SLP patterns associated with more local occurrence of extreme precipitation events. Verification of the RDA model performance for the periods 1961–1970 and 1991–2008 bestows highly unsatisfactory results. The area average correlation coefficients between observed and reconstructed d_{90} series are well below 0.5, and although it is not uncommon in the literature (Haylock et al. 2006), it suggests caution when performing downscaling procedures of extreme phenomena. Considerable differences in correlation coefficients between the calibration and validation period show that the identified relations might not be stationary, and possibly highlight the fact that the 20 yr period might not be long enough in the case of discrete phenomena such as rainfall extremes.

Acknowledgements. This study presents the outcomes of the research carried out as a part of the KLIMAT Project ('The influence of climate variability on the society, environment and economy') No. POIG.01.03.01-14-011/08-00 — a part of the Innovative Economy Operational Scheme co-financed by the European Fund for Regional Development.

LITERATURE CITED

Buishand TA, Shabalova MV, Brandsma T (2004) On the choice of temporal aggregation level for statistical downscaling of precipitation. J Clim 17:1816–1827

Busuioc A, Chen D, Hellström C (2001) Performance of statistical downscaling models in GCM validation and regional climate change estimates: application for Swedish precipitation. Int J Climatol 21:557–578

Busuioc A, Tomozeiu R, Cacciamani C (2008) Statistical downscaling model based on canonical correlation analysis for winter extreme precipitation events in the Emilia-Romagna region. Int J Climatol 28:449–464

Cavazos T, Hewitson BC (2005) Performance of NCEP-NCAR reanalysis variables in statistical downscaling of daily precipitation. Clim Res 28:95–107

Dobrowolski A, Ostrowski J, Żelaziński J (2005) Precipitation floods in Poland 1946–2001. In: Bogdanowicz E, Kossowska-Cezak U, Szkutnicki J (eds) Extreme hydrological and meteorological phenomena. Ser Monogr IMGW, IMGW i PTGeof, Warsaw, p 221–230 (in Polish)

Dubicki A, Słota H, Zieliński J (eds) (1999) Odra catchment: July 1997 flood monograph. IMGW, Warsaw (in Polish)

Goodess C, Alberghi S, Anagnostopoulou C, Bardossy A and others (2005) Recommendations on the more robust statistical and dynamical methods for construction of scenarios of extremes. Deliverable D16, Summary Rep version 2.0

Goodess CM, Anagnostopoulou C, Bardossy A, Frei C and others (2012) An intercomparison of statistical downscaling methods for Europe and European regions: assessing their performance with respect to extreme temperature and precipitation events. CRU RP11, University of East Anglia, Norwich

Grela J, Słota H, Zieliński H (eds) (1999) Vistula catchment:

July 1997 flood monograph. IMGW, Warsaw (in Polish)
Harpham C, Wilby RL (2005) Multi-site downscaling of heavy daily precipitation occurrence and amounts. J Hydrol 312:235–255
Haylock MR, Goodess CM (2004) Interannual variability of European extreme winter rainfall and links with mean large-scale circulation. Int J Climatol 24:759–776
Haylock MR, Cawley GC, Harpham C, Wilby RL, Goodess CM (2006) Downscaling heavy precipitation over the United Kingdom: a comparison of dynamical and statistical methods and their future scenarios. Int J Climatol 26: 1397–1415
Kalnay E, Kanamitsu M, Kistler R, Collins W and others (1996) The NCEP/NCAR 40-year Reanalysis Project. Bull Am Meteorol Soc 77:437–471
Klok EJ, Klein Tank AMG (2009) Updated and extended European dataset of daily climate observations. Int J Climatol 29:1182–1191
Kolendowicz L (2007) The influence of atmospheric circulation on the occurence of days with thunderstorm in Poland 1971–2000. In: Piotrowicz K, Twardosz R (eds) Climate variability in various spatial and temporal scales. Instytut Geografii i Gospodarki Przestrzennej UJ, Krakow, p 103–109 (in Polish)
Lorenc H (2005) Poland's climate atlas. IMGW, Warsaw
Łupikasza E (2010) Spatial and temporal variability of extreme precipitation in Poland in the period 1951–2006. Int J Climatol 30:991–1007
Makarenkov V, Legendre P (2002) Nonlinear redundancy analysis and canonical corresponce analysis based on polynominal regression. Ecology 83:1146–1161
Miętus M (1999) The role of atmospheric circulation over Europe and North Atlantic in forming climatic and oceanographic conditions in the Polish coastal zone. Materiały Badawcze IMGW, Ser Meteorol 29 (in Polish)
Miętus M, Filipiak J (2002) The influence of SST of the North Atlantic Ocean on the large-scale atmospheric circulation over the Atlantic Ocean and Europe and on the thermal conditions in Poland in the 20th century. Materiały Badawcze IMGW, Ser Meteorol 35 (in Polish)
Sauter T, Venema V (2011) Natural three-dimensional predictor domains for statistical precipitation downscaling. J Clim 24:6132–6145
Schmith T (2008) Stationarity of regression relationships: application to empirical downscaling. J Clim 21: 4529–4537
The WASA Group (1998) Changing waves and storms in the Northeast Atlantic? Bull Am Meteorol Soc 79:741–760
Twardosz R (1999) Maximum daily precipitation totals in Krakow 1863–1998 and their connection with synoptic situations. In: Changes and variability of the climate of Poland. National Scientific Conference, Łódź, p 269–273 (in Polish)
Tyler DE (1982) On the optimality of the simultaneous redundancy transformations. Psychometrika 47(1):77–86
von Storch H, Navarra A (eds) (1999) Analysis of climate variability. Applications of statistical techniques, 2nd edn. Springer-Verlag, Berlin
von Storch H, Zwiers FW (1999) Statistical analysis in climate research. Cambridge University Press, Cambridge
von Storch H, Zorita E, Cubasch U (1993) Downscaling of global climate change estimates to regional scales: an application to Iberian rainfall in wintertime. J Clim 6: 1161–1171
Wang XL, Zwiers FW (2001) Using redundancy analysis to improve dynamical seasonal mean 500 hPa geopotential forecasts. Int J Climatol 21:637–654
Werner PC, von Storch H (1993) Interannual variability of Central European mean temperature in January–February and its relation to large-scale circulation. Clim Res 3:195–207
Wilby RL, Wigley TML (2000) Precipitation predictors for downscaling: observed and general circulation model relationships. Int J Climatol 20(6):641–661
Zawiślak T (2005) Synoptic conditions of the occurence of intense precipitation events in south-western Poland on the basis of 2001–2003 period. In: Bogdanowicz E, Kossowska-Cezak U, Szkutnicki J (eds) Extreme hydrological and meteorological phenomena. Ser Monogr IMGW, IMGW i PTGeof, Warsaw, p 166–176 (in Polish)

Editorial responsibility: Balaji Rajagopalan, Boulder, Colorado, USA

Submitted: March 8, 2012; Accepted: February 11, 2013
Proofs received from author(s): April 26, 2013